University Library

MINERVA ACCESS

A gateway to Melbourne's research publications

Minerva Access is the Institutional Repository of The University of Melbourne

Author/s:
Holz, LE;Prier, JE;Freestone, D;Steiner, TM;English, K;Johnson, DN;Mollard, V;Cozijnsen, A;Davey, GM;Godfrey, DI;Yui, K;Mackay, LK;Lahoud, MH;Caminschi, I;McFadden, GI;Bertolino, P;Fernandez-Ruiz, D;Heath, WR

Title:
CD8+ T Cell Activation Leads to Constitutive Formation of Liver Tissue-Resident Memory T Cells that Seed a Large and Flexible Niche in the Liver

Date:
2018-10-02

Citation:
Holz, L. E., Prier, J. E., Freestone, D., Steiner, T. M., English, K., Johnson, D. N., Mollard, V., Cozijnsen, A., Davey, G. M., Godfrey, D. I., Yui, K., Mackay, L. K., Lahoud, M. H., Caminschi, I., McFadden, G. I., Bertolino, P., Fernandez-Ruiz, D. & Heath, W. R. (2018). CD8+ T Cell Activation Leads to Constitutive Formation of Liver Tissue-Resident Memory T Cells that Seed a Large and Flexible Niche in the Liver. Cell Reports, 25 (1), pp.68-79.e4. https://doi.org/10.1016/j.celrep.2018.08.094.

Persistent Link:
https://hdl.handle.net/11343/290373

License:
CC BY

Article

Cell Reports

CD8+ T Cell Activation Leads to Constitutive Formation of Liver Tissue-Resident Memory T Cells that Seed a Large and Flexible Niche in the Liver

Graphical Abstract

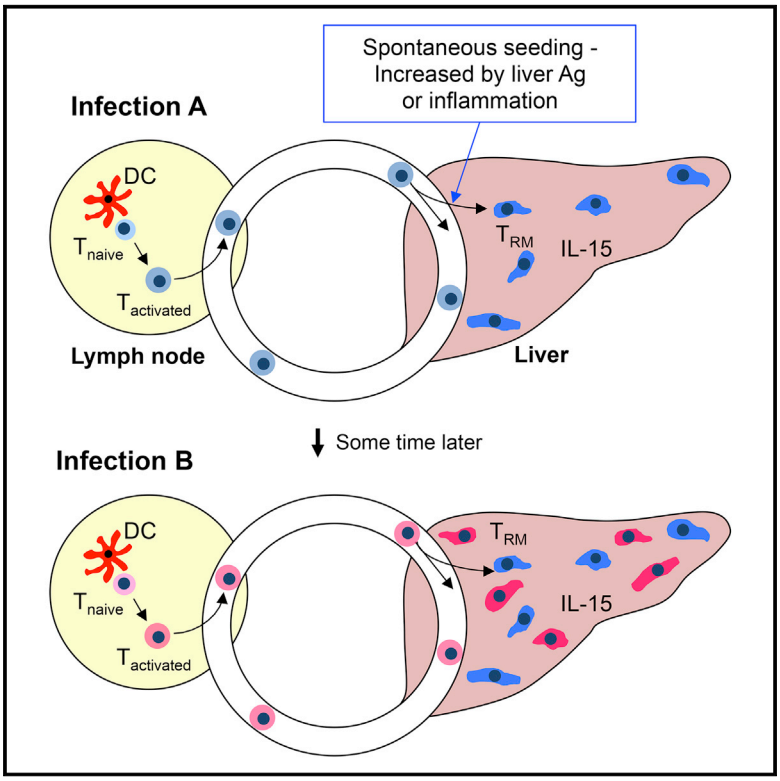

Authors

Lauren E. Holz, Julia E. Prier, David Freestone, ..., Patrick Bertolino, Daniel Fernandez-Ruiz, William R. Heath

Correspondence

lauren.holz@unimelb.edu.au (L.E.H.), danielfr@unimelb.edu.au (D.F.-R.), wrheath@unimelb.edu.au (W.R.H.)

In Brief

Holz et al. demonstrate that tissue-resident memory T (Trm) cells routinely develop in the liver after T cell activation. Within the liver, IL-15, antigen, and inflammation aid Trm cell formation, but only IL-15 is essential. Newly formed Trm cells do not displace existing populations, demonstrating a flexible liver niche.

Highlights

- TCR stimulation is essential for liver Trm cell formation
- Liver Trm cells require IL-15
- Local antigen presentation and inflammation enhance liver Trm cell formation
- Newly formed liver Trm cells do not displace existing Trm cell populations

Holz et al., 2018, Cell Reports *25*, 68–79
October 2, 2018 © 2018 The Author(s).
https://doi.org/10.1016/j.celrep.2018.08.094

OPEN ACCESS
CellPress

Cell Reports
Article

CD8+ T Cell Activation Leads to Constitutive Formation of Liver Tissue-Resident Memory T Cells that Seed a Large and Flexible Niche in the Liver

Lauren E. Holz,[1,2,*] Julia E. Prier,[1] David Freestone,[1] Thiago M. Steiner,[1] Kieran English,[3] Darryl N. Johnson,[1,2] Vanessa Mollard,[4] Anton Cozijnsen,[4] Gayle M. Davey,[1] Dale I. Godfrey,[1,2] Katsuyuki Yui,[5] Laura K. Mackay,[1,2] Mireille H. Lahoud,[6] Irina Caminschi,[6] Geoffrey I. McFadden,[4] Patrick Bertolino,[3] Daniel Fernandez-Ruiz,[1,*] and William R. Heath[1,2,7,*]

[1]Department of Microbiology and Immunology, Peter Doherty Institute for Infection and Immunity, University of Melbourne, Melbourne, VIC 3000, Australia
[2]ARC Centre of Excellence in Advanced Molecular Imaging, University of Melbourne, Parkville, VIC 3010, Australia
[3]Liver Immunology Program, Centenary Institute, and AW Morrow Gastroenterology and Liver Centre, The University of Sydney, Newtown, NSW 2042, Australia
[4]School of BioSciences, University of Melbourne, Parkville, VIC 3010, Australia
[5]Division of Immunology, Department of Molecular Microbiology and Immunology, Graduate School of Biomedical Sciences, Nagasaki University, 1-12-4 Sakamoto, Nagasaki 852-8523, Japan
[6]Infection and Immunity Program, Monash Biomedicine Discovery Institute and Department of Biochemistry and Molecular Biology, Monash University, Clayton, VIC 3800, Australia
[7]Lead Contact
*Correspondence: lauren.holz@unimelb.edu.au (L.E.H.), danielfr@unimelb.edu.au (D.F.-R.), wrheath@unimelb.edu.au (W.R.H.)
https://doi.org/10.1016/j.celrep.2018.08.094

SUMMARY

Liver tissue-resident memory T (Trm) cells migrate throughout the sinusoids and are capable of protecting against malaria sporozoite challenge. To gain an understanding of liver Trm cell development, we examined various conditions for their formation. Although liver Trm cells were found in naive mice, their presence was dictated by antigen specificity and required IL-15. Liver Trm cells also formed after adoptive transfer of *in vitro*-activated but not naive CD8+ T cells, indicating that activation was essential but that antigen presentation within the liver was not obligatory. These Trm cells patrolled the liver sinusoids with a half-life of 36 days and occupied a large niche that could be added to sequentially without effect on subsequent Trm cell cohorts. Together, our findings indicate that liver Trm cells form as a normal consequence of CD8+ T cell activation during essentially any infection but that inflammatory and antigenic signals preferentially tailor their development.

INTRODUCTION

Tissue-resident memory T cells are a recently described population of cells that are crucial for defense against pathogens at the site of infection (Schenkel and Masopust, 2014). As their name suggests, these cells do not recirculate like their effector memory T (Tem) and central memory T (Tcm) cell counterparts but, instead, remain localized within specific tissues (Jiang et al., 2012; Klonowski et al., 2004). This is in part due to their reduced expression of the sphingosine 1 phosphate (S1P) receptor (Mackay et al., 2015) and CCR7 (Wakim et al., 2012), both of which enable cells to migrate out of peripheral tissues into draining lymph nodes. Trm cells found in all tissues typically express the early activation marker CD69 and often CD103, but these markers do not precisely define Trm cells (Steinert et al., 2015). Regardless of their surface profiles, Trm cells found in all tissues express a core gene signature associated with residency, including the expression of *Hobit*, *Ctla4*, *Cdh1*, *Cdh2*, *Cd244*, and *Xcl1* (Mackay et al., 2013). Protection mediated by Trm cells has been associated with the production of cytokines, such as interferon-γ (IFN-γ) and tumor necrosis factor α (TNF-α), as well as markers of cytotoxicity, such as granzyme B and CD107a (Fernandez-Ruiz et al., 2016), indicating that these cells are poised to respond to immediate threats.

We have recently identified a population of Trm cells within the liver that are critical for protection from *Plasmodium* infection (malaria) (Fernandez-Ruiz et al., 2016). Large numbers of Trm cells were found in the liver after vaccination with radiation-attenuated sporozoites (RAS) or after a prime-and-trap vaccination approach, which utilizes priming with antigen targeted to Clec9A on conventional type 1 dendritic cells (cDC1s) combined with "trapping" of Trm cells in the liver upon recognition of hepatocyte-expressed antigen encoded by an adeno-associated viral vector. Trm cells generated by these vaccination strategies expressed high levels of the surface markers CD69, CXCR6, CXCR3, and CD101, but lacked expression of CD62L and KLRG1. Moreover, these Trm cells patrolled the liver sinusoids using a crawling motion that enabled scanning of hepatocytes for cognate antigen. The location of liver Trm cells in the sinusoids, which represent part of the blood stream, distinguishes these cells from most other Trm cells, which are found within parenchyma of peripheral tissues. Although both RAS vaccination and prime-and-trap vaccination provided protection against malaria, depletion of liver Trm cells from

 © 2018 The Author(s).
This is an open access article under the CC BY license (http://creativecommons.org/licenses/by/4.0/).

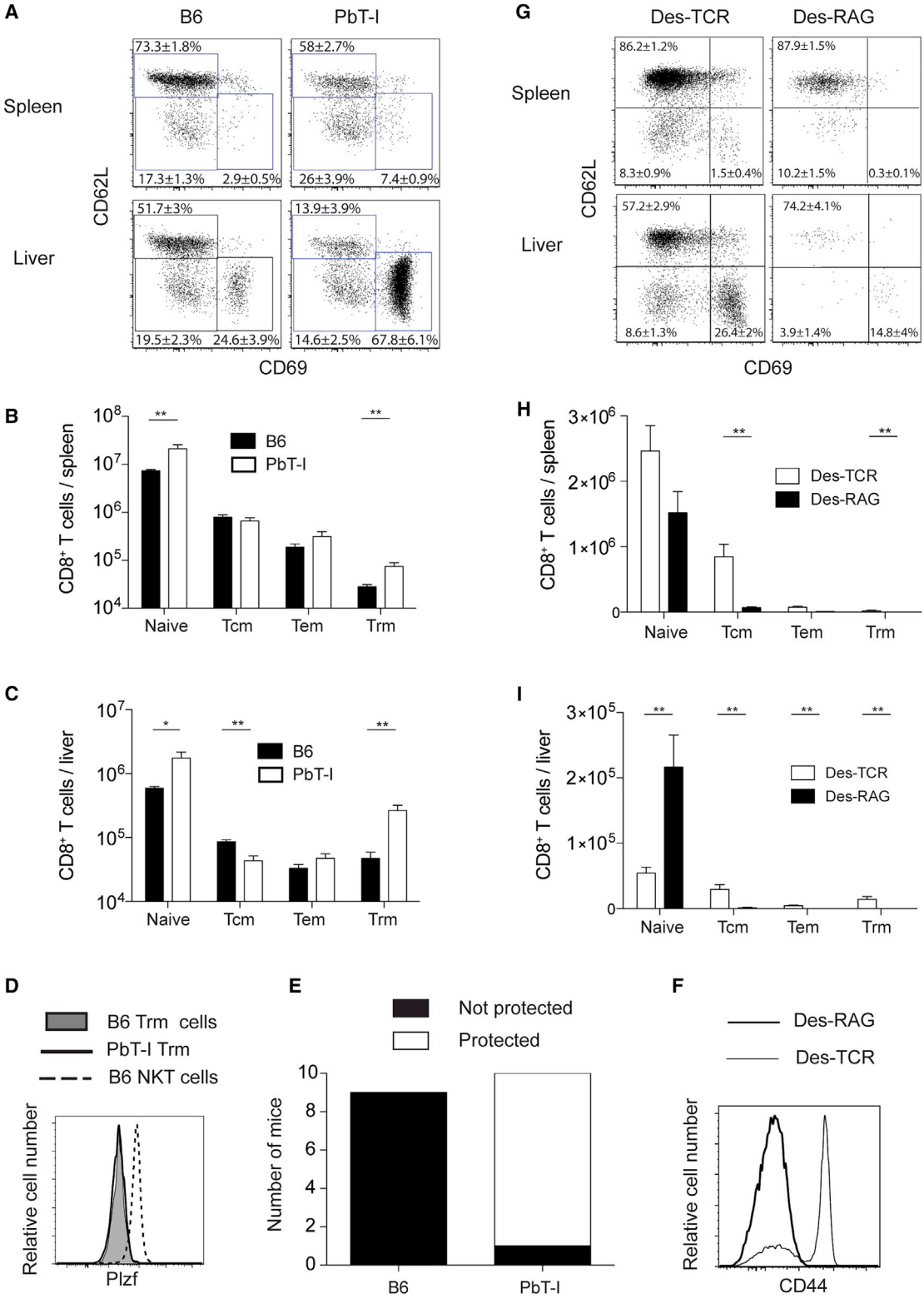

(legend on next page)

vaccinated mice by anti-CXCR3 antibody treatment abrogated protection, indicating an essential role of liver Trm cells in vaccine-mediated protection (Fernandez-Ruiz et al., 2016).

We and others have focused on the requirements for generating Trm cells so that maximum numbers can be formed, thereby enhancing immunity. In this study, we investigated the "spontaneous" formation of liver Trm cells in naive mice as well as the role of T cell activation in the establishment of liver Trm cell populations. We also investigated the size of the Trm cell niche in the liver by successively transferring different T cell populations intravenously to seed the liver. Our results show that we can expand the Trm cell population in the liver over 10-fold without altering the number of endogenous Trm cells. Combined, these data show that liver Trm cells develop naturally during the course of an immune response following T cell receptor (TCR) stimulation but that their numbers can be enhanced by liver infection or inflammation.

RESULTS

Liver Trm Cells Depend on Specific Antigen Recognition for Their Formation

As we previously reported (Fernandez-Ruiz et al., 2016), Trm cells ($CD44^{high}CD62L^{-}CD69^{+}$) can be identified in the livers of naive B6 mice (Figures 1A and 1C), raising the question of whether this memory population forms spontaneously or requires antigenic stimulation. To begin to address this question, we tested for the presence of Trm cells in the livers of naive TCR transgenic mice that had not been exposed to their specific antigen. PbT-I TCR transgenic mice, which express the $V\alpha8.3^{+}$ $V\beta10^{+}$ TCR specific for a K^{b}-restricted malaria antigen (Lau et al., 2014), were shown to contain both naive ($CD44^{low}$) and memory ($CD44^{high}$) $CD8^{+}$ T cell populations in their spleens and livers, with significant numbers of Trm cells in the liver (Figures 1A–1C). Such liver Trm cells in PbT-I transgenic mice expressed the $V\alpha$ and $V\beta$ chains of the transgenic TCR, as did similar Trm cell populations in several other TCR transgenic lines (i.e., OT-I, gBT-I, and P14), although the frequency and number of these cells varied between lines (Figure S1). This supported the possibility that liver Trm cells were able to form in the absence of antigenic stimulation, although the potential for activation through co-expressed recombined endogenous TCR in these lines hampered this conclusion. It was also noted that small numbers of T cells found in the spleen were detected as $CD44^{high}CD62L^{-}CD69^{+}$ (Figures 1A and 1B). Although splenic Trm cells have been reported previously (Schenkel et al., 2014), it was unclear whether the small population detected here were legitimate splenic Trm cells or simply background staining artifacts. Because these cells were not the focus of our study, we will cautiously refer to them as splenic Trm cells for the remainder of the paper but acknowledge that this is not definitive.

One trivial explanation for the presence of cells with a liver Trm cell phenotype ($CD44^{high}CD62L^{-}CD69^{+}$) in PbT-I mice (and other TCR transgenic lines) was that these cells were related to liver-resident natural killer T (NKT) cells, mucosal associated invariant T (MAIT) cells, or other unconventional T cells that had been forced to express the transgenic TCR. However, this did not appear to be the case because Trm cells found in PbT-I mice lacked expression of the transcription factor promyelocytic leukemia zinc finger (PLZF) (Figure 1D), confirming that they were different from NKT cells and MAIT cells.

Consistent with the presence of legitimate liver Trm cells in naive PbT-I mice, these mice were resistant to infection by *P. berghei* sporozoites (Figure 1E), which has been shown to depend on liver Trm cells (Fernandez-Ruiz et al., 2016).

Identification of *bona fide* liver Trm cells in PbT-I TCR transgenic mice raised the unlikely possibility that these cells formed spontaneously from a naive repertoire. An alternative explanation, however, was that their formation depended on co-expression of endogenously rearranged TCRs that enabled antigen-mediated activation and/or recruitment to the liver. To explore this possibility, we examined liver Trm cell formation in a second TCR transgenic mouse line, Des-TCR, which was specific for allogeneic K^{b}. These mice were available as either RAG-1-sufficient (termed Des-TCR) or RAG-1-deficient (termed Des-RAG), with the latter unable to rearrange endogenous receptors. Analysis of the spleens of these mice revealed that RAG-1-deficient mice contained very few $CD44^{high}$ memory T cells (Figures 1F–1H). Examination of memory T cell populations within the liver showed that Trm cells were only present in Des-TCR mice when endogenous receptor rearrangement was enabled (Figures 1G and 1I). A requirement for endogenous receptor rearrangement implied that antigen-specific responses to environmental antigens were required for formation of liver Trm cells, arguing against their spontaneous formation from naive T cells.

Figure 1. Trm Cells Form Spontaneously in Inbred and TCR Transgenic Mice

(A) Flow cytometry plots of $CD44^{high}$ memory $CD8^{+}$ T cells from the liver and spleen of naive B6 or PbT-I mice showing expression of CD62L and CD69.

(B and C) Total numbers (mean ± SEM are shown) of naive ($CD44^{low}$) and memory $CD8^{+}$ T cell subsets (Tcm cells [$CD44^{high}CD62L^{+}CD69^{-}$], Tem cells ($CD44^{high}CD62L^{-}CD69^{-}$], and Trm cells [$CD44^{high}CD62L^{-}CD69^{+}$]) in the spleen (B) and liver (C) of B6 and PbT-I mice. Results displayed are from 2 independent experiments using a total of 8 mice. See also Figure S1.

(D) Plzf expression in CD1d-αGal-Cer tetramer^{+} NKT cells from B6 mice (dashed line), and liver Trm cells from B6 (shaded) and PbT-I (solid line) mice.

(E) Number of B6 and PbT-I mice protected from infection after challenge with 200 PbA sporozoites. Results displayed are from 2 independent experiments using a total of 9–10 mice per group.

(F) Histogram of CD44 expression on total splenic $CD8^{+}$ T cells from Des-TCR (thin line) and Des-RAG (thick line) mice.

(G) Flow cytometry plots showing expression of CD69 and CD62L on $CD44^{high}$ memory $CD8^{+}$ T cells in the liver and spleen of naive Des-TCR and Des-RAG mice.

(H and I) Total numbers (mean ± SEM are shown) of naive ($CD44^{low}$) and memory $CD8^{+}$ T cell subsets in the spleen (H) and liver (I) of Des-TCR and Des-RAG mice. Results displayed are from 2 independent experiments using a total of 6–10 mice.

Groups were compared using Student's t test (B and C) or Mann-Whitney tests (H and I). $p < 0.05$ was considered significant. $^{**}p < 0.01$, $^{***}p < 0.001$, $^{****}p < 0.0001$.

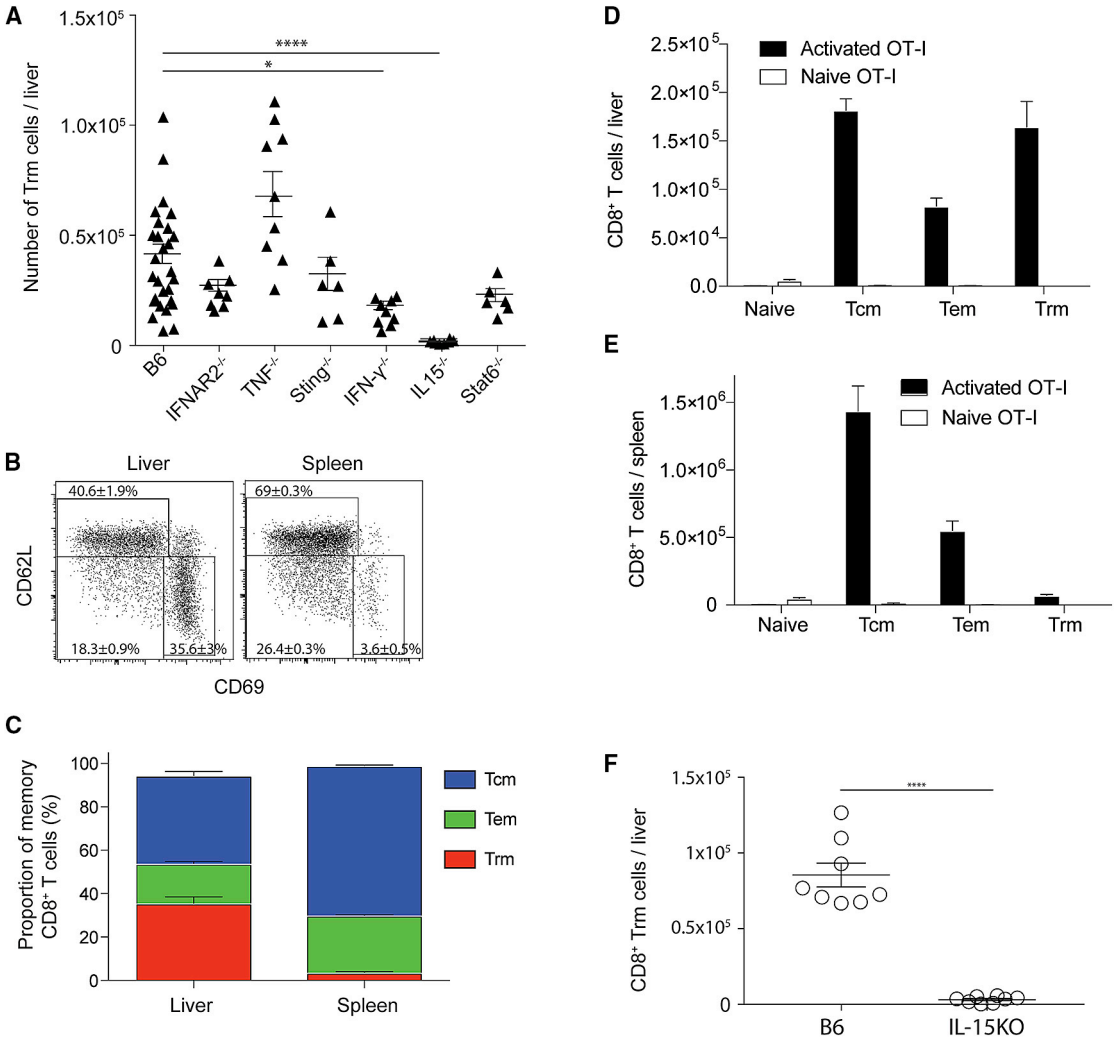

Figure 2. Trm Cells Depend on IL-15 and Form Spontaneously from Activated T Cells

(A) Naive B6, IFNAR2$^{-/-}$, TNF$^{-/-}$, Sting$^{-/-}$, IFN-γ$^{-/-}$, IL-15$^{-/-}$, and Stat6$^{-/-}$ mice were assessed for the number of endogenous Trm cells (CD8^{+}CD44^{high} CD62L^{-}CD69^{+}) in the liver. Results are pooled from multiple independent experiments with at least 2 experiments per knockout mouse line, using at least 3 mice per experiment. Symbols show individual mice, together with bars indicating mean ± SEM. Knockout mouse lines were compared with B6 mice using a Kruskal-Wallis test and Dunn's multiple comparison post-test. $p < 0.05$ was considered significant.

(B–E) 5 million *in vitro*-activated (B–E) or naive (D and E) OT-I.Ly5.1 cells were transferred into naive B6 mice. Livers (B–D) and spleens (B, C, and E) were harvested 2 weeks later, and the percentage (C) and number of naive and memory T cells (D and E) were assessed as in Figure 1. Results displayed are from 2 independent experiments using a total of 10 mice and show mean ± SEM. See also Figure S2.

(F) 20 million *in vitro*-activated OT-I.Ly5.1 cells were transferred into naive B6 or IL-15$^{-/-}$ mice. Livers were harvested 2 weeks later, and the number of memory T cells was assessed as in Figure 1. Symbols show individual mice, together with bars indicating mean ± SEM. Results displayed are from 2 independent experiments using a total of 8 mice. Groups were compared using an unpaired t test. $p < 0.05$ was considered significant.

*$p < 0.05$, ****$p < 0.0001$.

Liver Trm Cells Depend on IL-15

To explore the requirements for environmental antigen-triggered liver Trm cell formation in normal B6 mice, we screened various gene knockout mice for factors potentially important in liver Trm cell homeostasis. This analysis identified interleukin-15 (IL-15) as essential for the presence of liver Trm cells and also showed a minor effect of IFN-γ (Figure 2A). Cytokines such as tumor necrosis factor (TNF) and type I IFN had no significant effect on Trm cell formation, and lack of an effect in Stat6-deficient mice also implied that IL-4 signaling was not essential. These data suggested that endogenous liver Trm cells possessed a typical memory CD8^{+} T cell requirement for IL-15 but did not exclude a role for this cytokine in their development. Their requirement for IL-15 is explored further below.

Formation of Liver Trm Cells Occurs Constitutively from Activated T Cells

Although antigen recognition appeared to be essential for constitutive formation of liver Trm cells, it was unclear whether this was simply required to activate T cells or as an antigen recognition

step within the liver. To address this issue, we asked whether *in vitro*-activated TCR transgenic T cells could form liver Trm cells independent of antigen recognition within the liver. Ly5.1$^+$ ovalbumin (OVA)-specific TCR transgenic MHC I-restricted (OT-I) CD8$^+$ T cells (RAG-sufficient background) were activated with peptide *in vitro* and then transferred into naive B6 mice to assess liver Trm cell formation. After 2 weeks, livers and spleens were removed and examined for the presence of memory OT-I T cells based on expression of Ly5.1, CD44, CD62L, and CD69 (Figure 2B). This revealed formation of OT-I Trm cells (CD44^{high}CD62L$^-$CD69$^+$) in the livers of recipient mice, with the spleen containing predominantly Tem cells (CD44^{high}CD62L$^-$CD69$^-$) and Tcm cells (CD44$^+$CD62L$^+$CD69$^-$) (Figures 2B-E). By contrast, transferring naive OT-I T cells into naive B6 mice did not result in the formation of significant numbers of Trm cells. In fact, very few cells could be found in either the liver or spleen 2 weeks after this transfer (Figures 2D and 2E).

Our *in vitro* cultures used peptide, lipopolysaccharide (LPS), and IL-2 to generate large numbers of rapidly proliferating activated T cells for transfer. To test whether Trm cells could be generated in the absence of LPS and IL-2, we compared various activation conditions (Figure S2). OT-I T cells were activated under either neutral conditions (peptide alone or peptide + IL-15) or more inflammatory conditions (LPS with either IL-2 or IL-15). Liver Trm could be generated under all conditions, with the highest proportion generated by peptide alone (Figure S2A). Absolute Trm numbers, however, were highest in the livers of recipient mice receiving OT-I T cells activated in the presence of LPS (Figure S2B), as were total OT-I cell numbers in the spleen (Figure S2C). Thus, liver Trm cells formed irrespective of activation conditions, although the conditions that generated the most circulating memory cells also generated the largest number of liver Trm cells.

The ability to generate liver Trm cells from adoptively transferred *in vitro*-activated T cells allowed us to further explore the role of IL-15 in generating liver Trm cells. To assess this point, *in vitro*-activated OT-I cells were transferred into B6 or IL-15 knockout mice, and then liver Trm cell formation was measured 2 weeks later (Figure 2F). This showed that liver Trm cell formation was highly dependent on IL-15.

Combined, these findings suggested that liver Trm cells formed naturally from activated T cells in the presence of IL-15 and that neither antigen presentation in the liver nor inflammation of this tissue were essential for their formation.

Trm Cells Derived from *In Vitro*-Activated T Cells Patrol the Liver Sinusoids

To determine whether liver Trm cells derived from *in vitro*-activated T cells patrolled the liver sinusoids in a manner typical of previously reported liver Trm cells (Fernandez-Ruiz et al., 2016), mice ubiquitously expressing TdTomato were adoptively transferred with activated GFP-expressing OT-I cells and then, after several weeks, their livers were imaged, and cell migration was assessed (Figure 3A; Video S1). OT-I T cells within the liver showed a mean velocity of 8 μm/min (Figure 3B) and appeared to migrate within the liver sinusoids (Figure 3C). There was a mix of migration phenotypes, with about a quarter of the cells displaying the typical patrolling activity of liver Trm cells (Fernandez-Ruiz et al., 2016). The remaining OT-I T cells were non-patrolling, either rapidly flowing through the sinusoids or static, the latter suggesting temporary trapping within the tight confines of these narrow blood vessels (Figure 3D). The proportion of patrolling cells was similar to the proportion of Trm cells detected by flow cytometry in equivalent mice (Figures 2B and 2C). Because liver Trm cells have been shown to be essential for protection against sporozoite infection (Fernandez-Ruiz et al., 2016), we assessed whether memory OT-I cells formed by *in vitro* activation could provide such protection. To achieve this goal, mice containing liver Trm cells, derived from adoptive transfer of activated OT-I cells 3 weeks earlier, were challenged with live OVA-expressing *Plasmodium berghei* ANKA (PbA) sporozoites, and protection was assessed (Figure 3E). Complete protection against sporozoite challenge suggested that liver Trm cells formed after adoptive transfer were functional.

Lifespan and Limited Niche Competition by Liver Trm Cells

To determine the lifespan of liver Trm cells, 5×10^6 activated OT-I T cells were adoptively transferred into B6 mice and then left 14 to 100 days before harvesting livers and assessing Trm cell numbers. By plotting Trm cell number on a log scale and fitting a straight line to the data, we calculated a half-life of approximately 36 days, with a 95% confidence interval of 24–59 days (Figure 4A).

In earlier studies (Fernandez-Ruiz et al., 2016), we had measured Trm cell numbers generated by adoptively transferred malaria-specific PbT-I T cells at various times after vaccination with RAS. Although data points were relatively limited, cautioning over-interpretation, plotting these numbers on the same log scale revealed a similar decay rate of 28 days with a 95% confidence interval of 15–61 days (Figure 4A).

To gain an understanding of the nature of the liver Trm cell niche, we examined whether consecutive administration of activated T cells (and their subsequent formation of liver Trm cells) would enable seeding of increased numbers of liver Trm cells or whether the newly forming liver Trm cells would displace preexisting resident memory cells. To explore this question, 5×10^6 activated T cells were consecutively administered from three different TCR transgenic donors; i.e., OT-I, gBT-I, and P14, which recognize respective peptides from OVA, Herpes simplex virus type 1 (HSV) glycoprotein B, and lymphocytic choriomeningitis virus (LCMV) glycoprotein. Cells from each line were activated *in vitro* and then consecutively transferred into B6 hosts at 4-week intervals in the following order: OT-I, gBT-I, and P14. Four weeks after the final transfer, livers were harvested, and Trm cells were enumerated for each TCR transgenic population (Figure 4B). This showed that the number of OT-I Trm cells surviving to 12 weeks post-transfer was relatively small but unaffected by the subsequent introduction of gBT-I cells and then P14 cells. It also showed that the number of gBT-I Trm cells was unaffected by the later administration of P14 cells. Similarly, these data revealed that the endogenous Trm cell numbers were remarkably stable despite addition of up to three different TCR transgenic

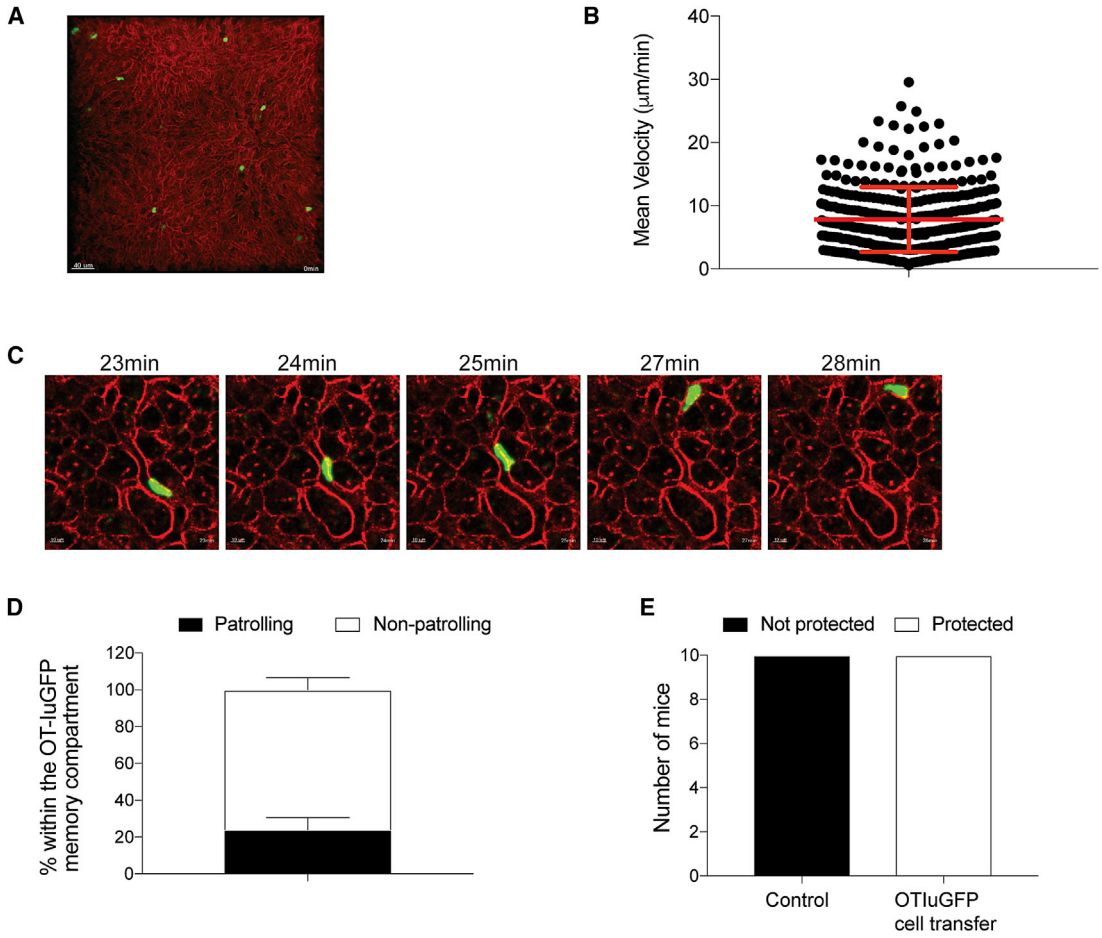

Figure 3. Liver Trm Cells Derived from *In Vitro*-Activated Cells Patrol in the Liver Sinusoids

20 million *in vitro*-activated GFP-expressing OT-I cells were transferred into naive TdTomato mice that ubiquitously express a membrane form of TdTomato. Intravital 2-photon microscopy of the liver was performed 2–4 weeks after cell transfer.

(A) Field of view of a 50-μm z stack. The scale bar represents 40 μm. See also Video S1.

(B) Mean velocity of individual OT-I cells. A total of 10 movies from 5 mice were analyzed. Mean velocity ± SD is shown in red.

(C) Single frames from intravital 2-photon imaging of GFP^+ OT-I cells within the liver of TdTomato mice over time. The scale bar represents 10 μm.

(D) Intravital 2-photon movies were quantitated for cells showing patrolling (crawling) behavior (black) or non-patrolling behavior (flowing in blood, sticking in sinusoids without crawling; white) (Fernandez-Ruiz et al., 2016). Mean ± SEM is shown, and a total of 10 movies from 5 mice were analyzed.

(E) Memory T cells formed by activated OT-I cells protect mice from challenge with OVA-expressing sporozoites. Naive B6 mice were injected with 20 million activated OT-I cells or left untreated. 3 weeks after transfer, mice were challenged with 200 OVA-expressing PbA sporozoites and monitored for parasitemia. Mice were considered protected when they remained negative for parasites by day 12. Results are from 2 independent experiments using a total of 10 mice per group.

cohorts. Overall, the total load of Trm cells increased nearly 5-fold in mice given a single type of transgenic T cell compared with those given all 3 consecutive populations.

To determine whether transferred cell numbers could be increased further to perhaps eventually fill the niche, we examined the number of liver Trm cells formed 4 weeks after injecting up to 40 × 10^6 activated T cells (Figure S3). This revealed that liver Trm cell numbers increased with an increasing dose but began to plateau after injection of 20 × 10^6 activated T cells. Given that 20 × 10^6 donor cells from a single injection induced the maximum number of Trm cells, we examined competition between the three TCR transgenic T cells cohorts when 20 × 10^6 activated cells were transferred at 2-week intervals (Figure 4C). Again, no evidence of competition was seen between consecutive populations, revealing a 10-fold increase in total Trm cell numbers in mice given all three populations. Similarly, OT-I Tcm and Tem cell populations were not reduced by addition of new transgenic populations (Figure S4).

To explore the potential for T cell competition in the liver niche after vaccination, *in vitro*-activated gBT-I cells were transferred into B6 mice, followed 3 weeks later by naive OT-I cells. Mice were then immunized with OVA conjugated to an anti-Clec9A antibody and adjuvanted by CpG (Caminschi et al., 2008). The generation of OT-I liver Trm cells by immunization did not alter the number of pre-existing gBT-I liver Trm cells (Figure 4D).

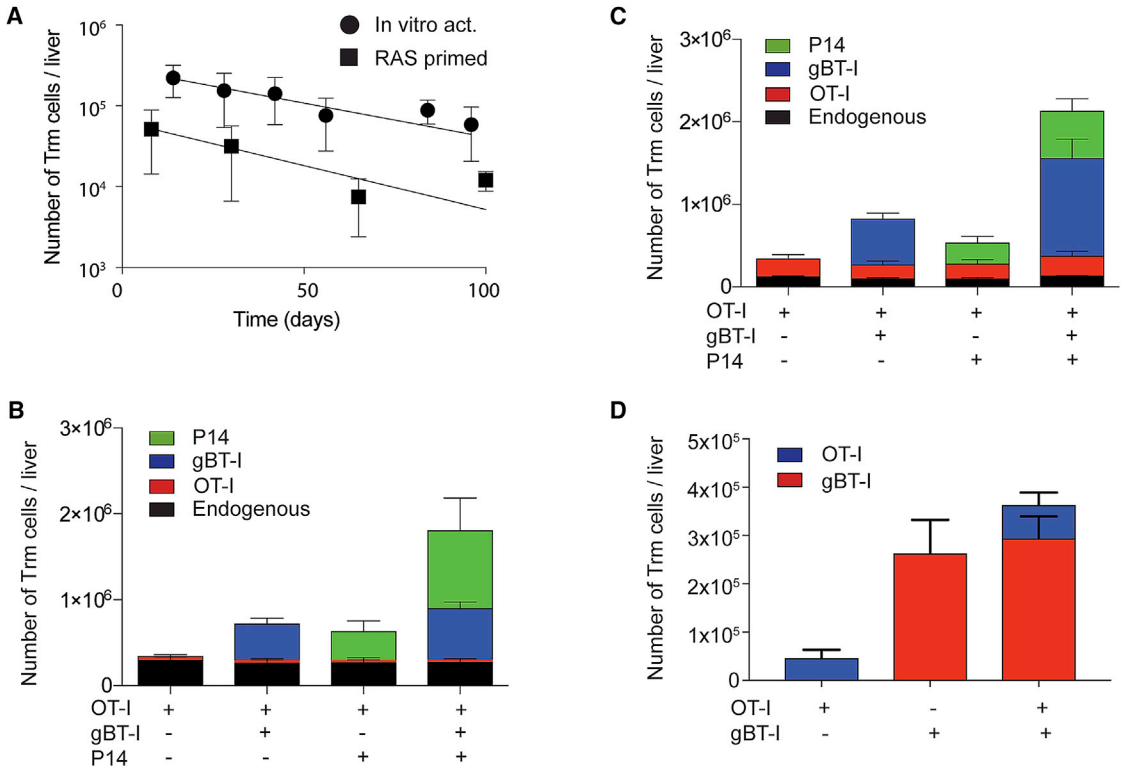

Figure 4. New Specificities Do Not Compete with Old Specificities for the Niche Occupied by Liver Trm Cells

(A) 5 million *in vitro*-activated OT-I.Ly5.1 CD8$^+$ T cells or 50,000 PbT-I.uGFP (ubiquitous green fluorescent protein) cells were transferred into naive B6 mice. Mice receiving PbT-I cells were vaccinated the following day with 50,000 RAS. Livers were harvested at various time points between 8 and 100 days, and total OT-I Trm (closed circles) and PbT-I Trm (closed squares) cell numbers were calculated. Data displayed are from 3 independent experiments using up to 15 mice per time point. Means ± SEM are shown. Half-life was calculated using an exponential growth equation in Prism 7.

(B) 5 million *in vitro*-activated OT-I, gBT-I, and P14 CD8$^+$ T cells were consecutively transferred into recipient mice at 4-week intervals, starting with OT-I at time point zero, gBT-I at 4 weeks, and P14 at 8 weeks. Some mice did not receive gBT-I cells or P14 T cells, as indicated by the symbols under the graph. Total Trm cell numbers were analyzed in the livers 4 weeks after P14 cell transfer. Means ± SEM are shown. Results displayed are from 2 independent experiments using a total of 10 mice per group.

(C) 20 million *in vitro*-activated OT-I, gBT-I, and P14 CD8$^+$ T cells were transferred into recipient mice as outlined in (B) but with 2-week intervals. Total Trm cell numbers were analyzed in the liver 2 weeks after the P14 cell transfer and revealed no change in endogenous and OT-I Trm numbers between groups (one way ANOVA and Tukey's multiple comparisons post-test). Results displayed are from 2 independent experiments using a total of 10 mice per group. Means ± SEM are shown. See also Figures S3 and S4.

(D) 20 million *in vitro*-activated gBT-I cells were transferred into naive B6 mice. 3 weeks later, 50,000 naive OT-I.Ly5.1 cells were transferred into the mice and primed the following day using CpG B-P (CpG 2006-21798) and anti-Clec9A-OVA. Some mice did not receive gBT-I cells or OT-I T cells, as indicated by the symbols under the graph. Livers were harvested from all groups 3 weeks following OT-I priming, and Trm numbers were assessed. Results displayed are from 2 independent experiments using a total of 10 mice per group. Means ± SEM are shown. No significant difference was observed.

Combined, these data suggested that the niche available for liver Trm cell formation was relatively large (exceeding 2 million Trm cells per liver) and that consecutive seeding of populations simply added to existing liver Trm cells.

Formation of Liver Trm Cells Occurs after Infection

The above findings suggested that liver Trm cells would be generated from any CD8$^+$ T cell population activated during the course of an infection. To examine this possibility, we adoptively transferred 50,000 naive PbT-I T cells into B6 mice and then measured memory T cell populations in the spleen and liver after infection with either blood-stage PbA, which does not infect liver cells, or with PbA RAS, which infect hepatocytes. This revealed that both infection conditions induced liver Trm cell formation (Figures 5A and 5B). However, comparison of the ratio of liver Trm cells to circulating memory T cells (Tcirc; total Tem cells plus Tcm cells from the spleen) showed a bias toward Trm cell formation after RAS infection (Figure 5D). This difference was also reflected in total liver Trm cell numbers, which were also higher after RAS vaccination, despite infected red blood cells (iRBCs) inducing more circulating memory T cells in the spleen (Figure S5). These findings suggested that, although Trm cells can form spontaneously in the liver following TCR stimulation, factors such as antigen and/or inflammation associated with liver infection may influence the extent of their formation. This is consistent with our earlier observation that expression of antigen in the liver favored formation of liver Trm cells after prime-and-trap vaccination (Fernandez-Ruiz et al., 2016).

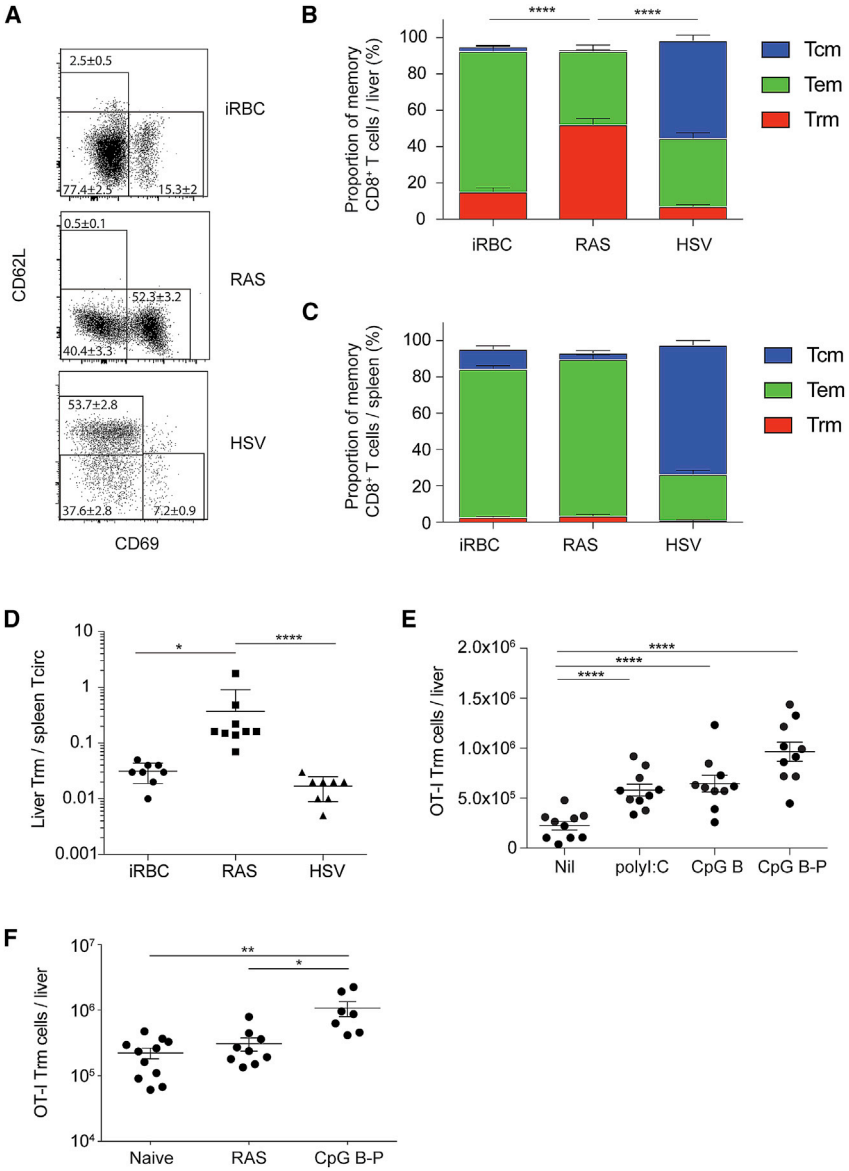

Figure 5. Liver Infection and/or Inflammation Enhances Liver Trm Formation

(A–C) Mice received 50,000 PbT-I cells prior to infection with iRBC or vaccination with 50,000 RAS, or mice received 1 million gBT-I cells prior to infection with HSV. On days 60–65, livers (A and B) and spleens (C) were harvested and analyzed by flow cytometry to determine the proportion of Tcm, Tem, and Trm cells. See also Figure S5.

(D) The number of Trm cells in the liver was divided by the number of circulating T cells in the spleen (Tem cells and Tcm cells) to calculate the relative proportion of Trm cells in the liver.

Results for (A)–(D) are from 2 independent experiments using a total of 8 mice. Means ± SEM are shown. Groups were compared using a Kruskal-Wallis test with Dunn's multiple comparison post-test in (D), and Trm percentages in (B) and (C) were compared using one way ANOVA with Tukey's multiple comparisons post-test. $p < 0.05$ was considered significant.

(E) Inflammatory signals enhance liver Trm cell formation. 5 million *in vitro*-activated OT-I cells were transferred into naive B6 mice alone or in the presence of the adjuvants poly(I:C), CpG B (CpG 1668), or CpG B-P (CpG 2006-21798). Livers were harvested 3 weeks later, and the number of OT-I Trm cells was determined by flow cytometry. Results displayed are from 2 independent experiments using a total of 10 mice. Values for individual mice and means ± SEM are shown. Groups were compared by one-way ANOVA and Tukey's multiple comparisons test, and $p < 0.05$ was considered significant.

(F) Inflammatory signals derived from RAS are not sufficient to enhance liver Trm cell formation. Mice were pre-treated with CpG B-P or 50,000 RAS 2 hr prior to the transfer of 10 million *in vitro*-activated OT-I cells. Livers and spleens were harvested on days 30–31, and OT-I Trm cells were enumerated. Data are pooled from 2 independent experiments using 3–6 mice per experiment. Values for individual mice and means ± SEM are shown. Groups were compared using a Kruskal-Wallis test with Dunn's multiple comparison post-test, and $p < 0.05$ was considered significant.

*$p < 0.05$, **$p < 0.01$, ***$p < 0.001$.

Because blood-stage infection with *P. berghei* can cause some liver inflammation, as measured by the release of acute-phase proteins (Ansar et al., 2009; Friedman, 1983), and inflammation has been shown to help Trm cell formation in various tissues (Fernandez-Ruiz et al., 2016; Mackay et al., 2012; Wakim et al., 2010), this may have contributed to seeding of Trm cells in the liver during blood-stage infection. To investigate whether liver Trm cells would form after an infection not known to cause liver inflammation, we examined Trm cell formation after cutaneous infection with HSV. One million naive TCR transgenic T cells from the HSV-specific gBT-I line were adoptively transferred into B6 mice that were then infected with HSV by skin scarification. Mice were left 60–65 days before measuring memory cell formation in the liver and spleen (Figures 5A–5C). Liver Trm cells clearly formed after HSV infection, but their proportion relative to circulating memory was lower than seen for malaria (Figure 5D). The absolute number of liver Trm cells in this case was comparable to RAS vaccination (Figure S5), although, overall, much greater responses were induced. This may relate to the greater number of naive gBT-I cells used to monitor this response or to differences in the infections. Together, these data implied that liver Trm cells formed even after infections that did not involve the liver but that inflammation and/or antigen may optimize seeding.

Inflammatory Stimuli Boost Liver Trm Cell Numbers

To examine the role of inflammatory stimuli on the formation of liver Trm cells, B6 mice were adoptively transferred with activated OT-I cells alone or together with an inflammatory stimulus in the form of poly(I:C), a Toll-like receptor (TLR) 3 agonist, or one of two different types of CpG, which are TLR9 agonists. These mice were then left for 3 weeks before harvesting their livers

and assessing liver Trm cell numbers (Figure 5E). This revealed that addition of inflammatory stimuli significantly increased liver Trm cell formation, with CpG B-P being the most potent. CpG B-P is comprised of a B class oligodeoxynucleotide (ODN, 2006) linked to a P class ODN (21798), which, we have found, is a more effective adjuvant for inducing $CD8^+$ T cell immunity than the single components alone (unpublished data).

Given that inflammatory stimuli increase liver Trm cell numbers, and RAS administration has been reported to induce inflammatory signals in the liver (Liehl et al., 2014; Miller et al., 2014), we asked whether the increase in liver Trm cells seen with RAS vaccination may be a consequence of RAS-induced inflammation. Naive B6 mice were injected with activated OT-I cells (a non-specific T cell population that could not recognize antigen on sporozoites) and also injected with RAS or CpG B-P. Three weeks later, liver Trm cell numbers were assessed (Figure 5F). This indicated that, unlike CpG B-P, co-administration of RAS was unable to increase liver Trm cell numbers relative to untreated controls. These findings suggest that formation of parasite-specific Trm cells in response to RAS vaccination is not mediated by inflammatory signals. Given that RAS generate substantial Trm cells compared with other forms of priming, this finding implicates antigenic signals associated with RAS, rather than inflammatory signals, as important for Trm cell formation by this form of priming.

DISCUSSION

Trm cells have been described in many non-lymphoid tissues (reviewed in Schenkel and Masopust, 2014). Here we focused on liver Trm cells and show that these cells form after TCR stimulation in naive inbred mice as well as naturally during the course of an immune response. IL-15 expression is critical for the development of these cells because mice deficient in IL-15 lack endogenous liver Trm cells, and *in vitro* activated cells cannot form liver Trm cells in IL-15 knockout mice. Previous studies have found that the IL-15 dependence of Trm cells varies between tissues, with those in the skin, salivary gland, and kidney heavily dependent on this cytokine, whereas others, in tissues such as the female reproductive tract and small intestine, are independent (Mackay et al., 2013; Schenkel et al., 2016). Our studies do not distinguish between an IL-15 requirement for development, maintenance, or homeostatic proliferation, but IL-15 has been shown to contribute to all three aspects of the memory T cell life cycle in other tissues (Berard et al., 2003; Greyer et al., 2016; Schenkel et al., 2016), leaving multiple contributions possible.

Unlike Trm cells found in most organs, liver Trm cells induced by vaccination or infection do not reside within epithelial tissues or other parenchyma but, instead, patrol the liver sinusoids (Fernandez-Ruiz et al., 2016; Masopust et al., 2010). Here we show that liver Trm cells generated by adoptive transfer, like those induced by other means, migrate within the sinusoids and are able to control sporozoite infection. Given the relatively large volume of the liver and its extensive sinusoidal network, we asked whether there was a limit to the number of Trm cells that could occupy this organ. Successive adoptive transfer of *in vitro*-activated T cells increased the total number of Trm cells by up to 10-fold, reaching around 2 million cells, with successive transfers having little effect on previously formed populations that occupy the same niche. Moreover, generation of Trm cells by vaccination did not affect Trm cells already present in the liver. Consistent with our observations in the liver, sites such as the salivary gland and female reproductive tract are able to accommodate 50-fold more Trm cells when immunized on three successive occasions compared with once (Schenkel et al., 2016). Lack of competition between Trm cell cohorts may not always be the case, however, because some level of competition between skin Trm cells was noted during MVA infection, where certain antigen specificities could be outcompeted by immunodominant or high-frequency precursors (Muschaweckh et al., 2016). In general, however, the limited competition of Trm cells in sites like the liver, female reproductive tract, and salivary glands suggest that multiple vaccinations could generate large pools of patrolling cells specific for several local pathogens without altering the pre-existing T cell pool.

Although Trm cell formation within an organ is not always dependent on infection of that organ (Jiang et al., 2012; Masopust et al., 2010), two factors have a major effect on the differentiation and seeding of Trm cells within tissues during an immune response: local antigen presentation (Davies et al., 2017; Fernandez-Ruiz et al., 2016; Khan et al., 2016) and inflammation (Mackay et al., 2012). The latter may exert its effect by upregulation of chemokines such as CXCL10, which attract Trm cell precursors (Nakanishi et al., 2009). Our study shows that local antigen presentation is not necessary for the accumulation of Trm cells in the liver because transferring *in vitro*-activated $CD8^+$ T cells into naive mice led to the accumulation of large numbers of Trm cells in this organ. Although we have previously reported enhanced liver Trm cell formation in the presence of inflammatory stimuli or antigen (Fernandez-Ruiz et al., 2016), this earlier work could not isolate antigenic effects from inflammatory effects because both antigen and adjuvant were co-administered. Here we show that, in the absence of any antigenic stimuli *in vivo*, liver Trm cell formation is increased by the presence of inflammatory signals generated by poly(I:C) or CpG adjuvants, with CpG B-P having a moderately greater effect than the other adjuvants. Use of CpG B-P was based on the observation that DEC205 contributes to the uptake of B class CpG ODN by dendritic cells, improving their potency (Caminschi et al., 2013), whereas P class CpG ODNs do not bind DEC205 (unpublished data). Because P class ODNs more efficiently trigger production of type I IFN, IL-6, and the CXCR3 ligand CXCL10 (Samulowitz et al., 2010), we fused a DEC205-binding B class ODN to a P class ODN to form a CpG B-P ODN that would bind DEC205 to facilitate uptake by dendritic cells and then utilize the superior cytokine-inducing properties of the P class ODN. Future experiments will assess the precise factors that contributed to the improved liver Trm cell formation in the presence of CpG B-P.

The increase in Trm cell numbers caused by co-administration of adjuvant is consistent with previous data generated in a skin model, which found that administration of the inflammatory agent 1-fluoro-2,4-dinitrobenzene (DNFB) on the skin was necessary for the recruitment of cells that formed Trm cells within this tissue (Mackay et al., 2012). Similar observations

were made for gut Trm cell development in a model of *Yersinia pseudotuberculosis* infection (Bergsbaken and Bevan, 2015). In this case, infection-derived inflammation was required for the recruitment of Trm cells into the *lamina propria* in a process that was dependent on CXCR3 expression by responding T cells.

Unlike other non-lymphoid tissues, however, there is limited need to specifically recruit T cells to the liver for formation of resident memory because the entire blood volume passes through the liver every few minutes (Greenway and Stark, 1971). In tissues like the skin, Trm cell precursors are required to leave the blood and access parenchymal environments before they fully develop into Trm cells. Because liver Trm cells are localized within the sinusoids, circulating precursors have direct access to the liver Trm cell niches without egress from the blood. Thus, although chemokine-dependent recruitment may contribute to increased Trm cell formation in the liver after administration of adjuvants, it is worth considering alternative mechanisms. Enhanced Trm cell formation in the presence of CpG ODNs may relate to proliferation of $CD8^+$ T cells within the liver because CpG adjuvants have been reported to induce intrahepatic myeloid cell aggregates (iMATEs) that support local $CD8^+$ T cell proliferation (Huang et al., 2013). Such iMATEs are not induced by poly(I:C) (Huang et al., 2013), however, suggesting that this adjuvant may supply alternative signals, such as type I IFN, that influence Trm cell recruitment, development, or even retention.

Because interactions between integrins or chemokine receptors and their ligands make important contributions to $CD8^+$ T cell responses in the liver (Bertolino et al., 2005; Lee and Kubes, 2008; McNamara et al., 2017; Tse et al., 2014), alterations in these receptor-ligand pairs may be important. Retention of liver-resident NKT cells, which, like $CD8^+$ Trm cells, also patrol the sinusoids, relies on interactions between CXCR6 expressed on NKT cells and CXCL16 expressed on liver sinusoidal endothelial cells (LSECs) (Geissmann et al., 2005). Liver Trm cells express CXCR6 (Fernandez-Ruiz et al., 2016), and $CD8^+$ T cells deficient for this receptor form memory T cells poorly in the liver (Tse et al., 2014), implicating this interaction in Trm cell maintenance. LFA-1 expressed by liver Trm cells and its interaction with ICAM-1 expressed on hepatocytes and/or LSECs has also been shown to be critical for retention of these T cells in the liver (McNamara et al., 2017). Because the expression of receptor-ligand pairs such as these can be affected by cytokines induced by CpG or poly(I:C) (Murray et al., 2016; Sacher et al., 2002; Tohyama et al., 2007; Wuttge et al., 2004), it is feasible that initial retention of precursors within the liver sinusoids is mediated by adjuvants, leading to greater Trm cell formation.

Evidence that RAS vaccination promotes more efficient liver Trm cell formation than either HSV skin infection or blood-stage PbA infection suggests that infection of the liver is key to generating efficient responses in this tissue. This does not appear to be due to increased inflammation of the liver because co-administration of activated non-specific OT-I T cells with a vaccine dose of RAS failed to increase liver Trm cell formation. Given the large number of sporozoites used and the documented inflammatory signals arising from this type of vaccination (Liehl et al., 2014; Miller et al., 2014), this observation was somewhat surprising. Importantly, however, with respect to vaccine development, it implies that potential additional benefits might be gained by combining alternative inflammatory signals with RAS vaccination. In this light, adding α-galactosylceramide (αGalCer), an NKT cell stimulus, to RAS has been reported to improve vaccine efficacy (Gonzalez-Aseguinolaza et al., 2000). It will be interesting to explore the ideal adjuvants for facilitating optimal liver Trm cell formation when combined with RAS.

Combined, we show that liver Trm cells form after TCR stimulation in mice, generating a population of endogenous cells that have the capacity to mount an immune response. These cells will also form during the natural course of an immune response, and their numbers can be enhanced by the presence of local antigen and inflammation. Finally, we reveal the considerable size of the liver niche, indicating that there is limited competition between immune subsets.

STAR★METHODS

Detailed methods are provided in the online version of this paper and include the following:

- KEY RESOURCES TABLE
- CONTACT FOR REAGENT AND RESOURCE SHARING
- EXPERIMENTAL MODEL AND SUBJECT DETAILS
  - Mice
  - Ethics statement
  - Plasmodium Infection
- METHODS DETAILS
  - Vaccination
  - *In vitro* T cell activation and transfer
  - Lymphocyte isolation from organs
  - Flow cytometry
  - Intravital 2 photon microscopy
- QUANTIFICATION AND STATISTICAL ANALYSIS
  - Statistical analysis

SUPPLEMENTAL INFORMATION

Supplemental Information includes five figures and one video and can be found with this article online at https://doi.org/10.1016/j.celrep.2018.08.094.

ACKNOWLEDGMENTS

We thank the BRF facility at the Peter Doherty Institute and the Centenary Institute Animal Facility and Advanced Cytometry Facility for technical support. We also thank Dr. John Cambier for providing the Sting knockout mice. L.E.H., D.N.J., and D.I.G. were supported by the Australian Research Council (Centre for Advanced Molecular Imaging). J.E.P., D.F., and L.K.M. were supported by an NHMRC program grant (APP1129711). D.F.-R., T.M.S., and G.D. were supported by an NHMRC program grant (APP1113293). W.R.H. was supported by an NHMRC fellowship (APP1059861). D.I.G. was supported by an NHMRC Senior Principal Research Fellowship (APP1117766). K.E. and P.B. were supported by NHMRC (project grants APP1108565 and APP1086451). G.I.M. was supported by an NHMRC project grant and an ARC Discovery Project and Laureate Fellowship.

AUTHOR CONTRIBUTIONS

Conceptualization, W.R.H., L.E.H., and D.F.-R.; Methodology, W.R.H., K.Y., I.C., M.H.L., and D.F.-R.; Investigation, L.E.H., J.E.P., D.F., T.M.S., K.E.,

A.C., G.M.D., and D.F.-R.; Writing – Original Draft, L.E.H. and W.R.H.; Writing – Review & Editing, L.E.H., J.E.P., D.F., T.M.S., K.E., D.N.J., V.M., A.C., G.M.D., D.I.G., K.Y., L.K.M., M.H.L., I.C., G.I.M., P.B., D.F.-R., and W.R.H.; Funding Acquisition, D.I.G., L.K.M., I.C., G.I.M., P.B., and W.R.H.; Resources, D.N.J., V.M., A.C., D.I.G., K.Y., L.K.M., M.H.L., G.I.M., and I.C.; Supervision, D.I.G., L.K.M., M.H.L., I.C., G.I.M., P.B., and W.R.H.

DECLARATION OF INTERESTS

The authors declare no competing interests.

Received: December 19, 2017
Revised: July 23, 2018
Accepted: August 30, 2018
Published: October 2, 2018

REFERENCES

Ansar, W., Habib, S.K., Roy, S., Mandal, C., and Mandal, C. (2009). Unraveling the C-reactive protein complement-cascade in destruction of red blood cells: potential pathological implications in Plasmodium falciparum malaria. Cell. Physiol. Biochem. *23*, 175–190.

Benedict, M.Q. (1997). Care and maintenance of anopheline mosquito colonies. In The Molecular Biology of Insect Disease Vectors: A Methods Manual, J.M. Crampton, C.B. Beard, and C. Louis, eds. (Dordrecht: Springer Netherlands), pp. 3–12.

Berard, M., Brandt, K., Bulfone-Paus, S., and Tough, D.F. (2003). IL-15 promotes the survival of naive and memory phenotype CD8+ T cells. J. Immunol. *170*, 5018–5026.

Bergsbaken, T., and Bevan, M.J. (2015). Proinflammatory microenvironments within the intestine regulate the differentiation of tissue-resident CD8$^+$ T cells responding to infection. Nat. Immunol. *16*, 406–414.

Bertolino, P., Schrage, A., Bowen, D.G., Klugewitz, K., Ghani, S., Eulenburg, K., Holz, L., Hogg, N., McCaughan, G.W., and Hamann, A. (2005). Early intrahepatic antigen-specific retention of naïve CD8+ T cells is predominantly ICAM-1/LFA-1 dependent in mice. Hepatology *42*, 1063–1071.

Caminschi, I., Proietto, A.I., Ahmet, F., Kitsoulis, S., Shin Teh, J., Lo, J.C., Rizzitelli, A., Wu, L., Vremec, D., van Dommelen, S.L., et al. (2008). The dendritic cell subtype-restricted C-type lectin Clec9A is a target for vaccine enhancement. Blood *112*, 3264–3273.

Caminschi, I., Meuter, S., and Heath, W.R. (2013). DEC-205 is a cell surface receptor for CpG oligonucleotides. OncoImmunology *2*, e23128.

Dalton, D.K., Pitts-Meek, S., Keshav, S., Figari, I.S., Bradley, A., and Stewart, T.A. (1993). Multiple defects of immune cell function in mice with disrupted interferon-gamma genes. Science *259*, 1739–1742.

Davies, B., Prier, J.E., Jones, C.M., Gebhardt, T., Carbone, F.R., and Mackay, L.K. (2017). Cutting Edge: Tissue-Resident Memory T Cells Generated by Multiple Immunizations or Localized Deposition Provide Enhanced Immunity. J. Immunol. *198*, 2233–2237.

Fenner, J.E., Starr, R., Cornish, A.L., Zhang, J.G., Metcalf, D., Schreiber, R.D., Sheehan, K., Hilton, D.J., Alexander, W.S., and Hertzog, P.J. (2006). Suppressor of cytokine signaling 1 regulates the immune response to infection by a unique inhibition of type I interferon activity. Nat. Immunol. *7*, 33–39.

Fernandez-Ruiz, D., Ng, W.Y., Holz, L.E., Ma, J.Z., Zaid, A., Wong, Y.C., Lau, L.S., Mollard, V., Cozijnsen, A., Collins, N., et al. (2016). Liver-resident memory CD8+ T cells form a front-line defense against malaria liver-stage infection. Immunity *45*, 889–902.

Friedman, M.J. (1983). Control of malaria virulence by alpha 1-acid glycoprotein (orosomucoid), an acute-phase (inflammatory) reactant. Proc. Natl. Acad. Sci. USA *80*, 5421–5424.

Gebhardt, T., Wakim, L.M., Eidsmo, L., Reading, P.C., Heath, W.R., and Carbone, F.R. (2009). Memory T cells in nonlymphoid tissue that provide enhanced local immunity during infection with herpes simplex virus. Nat. Immunol. *10*, 524–530.

Geissmann, F., Cameron, T.O., Sidobre, S., Manlongat, N., Kronenberg, M., Briskin, M.J., Dustin, M.L., and Littman, D.R. (2005). Intravascular immune surveillance by CXCR6+ NKT cells patrolling liver sinusoids. PLoS Biol. *3*, e113.

Gonzalez-Aseguinolaza, G., de Oliveira, C., Tomaska, M., Hong, S., Bruna-Romero, O., Nakayama, T., Taniguchi, M., Bendelac, A., Van Kaer, L., Koezuka, Y., and Tsuji, M. (2000). alpha -galactosylceramide-activated Valpha 14 natural killer T cells mediate protection against murine malaria. Proc. Natl. Acad. Sci. USA *97*, 8461–8466.

Greenway, C.V., and Stark, R.D. (1971). Hepatic vascular bed. Physiol. Rev. *51*, 23–65.

Greyer, M., Whitney, P.G., Stock, A.T., Davey, G.M., Tebartz, C., Bachem, A., Mintern, J.D., Strugnell, R.A., Turner, S.J., Gebhardt, T., et al. (2016). T Cell Help Amplifies Innate Signals in CD8(+) DCs for Optimal CD8(+) T Cell Priming. Cell Rep. *14*, 586–597.

Hammond, K.J., Pellicci, D.G., Poulton, L.D., Naidenko, O.V., Scalzo, A.A., Baxter, A.G., and Godfrey, D.I. (2001). CD1d-restricted NKT cells: an inter-strain comparison. J. Immunol. *167*, 1164–1173.

Hogquist, K.A., Jameson, S.C., Heath, W.R., Howard, J.L., Bevan, M.J., and Carbone, F.R. (1994). T cell receptor antagonist peptides induce positive selection. Cell *76*, 17–27.

Hua, C., Boyer, C., Buferne, M., and Schmitt-Verhulst, A.M. (1986). Monoclonal antibodies against an H-2Kb-specific cytotoxic T cell clone detect several clone-specific molecules. J. Immunol. *136*, 1937–1944.

Huang, L.R., Wohlleber, D., Reisinger, F., Jenne, C.N., Cheng, R.L., Abdullah, Z., Schildberg, F.A., Odenthal, M., Dienes, H.P., van Rooijen, N., et al. (2013). Intrahepatic myeloid-cell aggregates enable local proliferation of CD8(+) T cells and successful immunotherapy against chronic viral liver infection. Nat. Immunol. *14*, 574–583.

Jiang, X., Clark, R.A., Liu, L., Wagers, A.J., Fuhlbrigge, R.C., and Kupper, T.S. (2012). Skin infection generates non-migratory memory CD8+ T(RM) cells providing global skin immunity. Nature *483*, 227–231.

Jin, L., Hill, K.K., Filak, H., Mogan, J., Knowles, H., Zhang, B., Perraud, A.L., Cambier, J.C., and Lenz, L.L. (2011). MPYS is required for IFN response factor 3 activation and type I IFN production in the response of cultured phagocytes to bacterial second messengers cyclic-di-AMP and cyclic-di-GMP. J. Immunol. *187*, 2595–2601.

Kaplan, M.H., Schindler, U., Smiley, S.T., and Grusby, M.J. (1996). Stat6 is required for mediating responses to IL-4 and for development of Th2 cells. Immunity *4*, 313–319.

Kennedy, M.K., Glaccum, M., Brown, S.N., Butz, E.A., Viney, J.L., Embers, M., Matsuki, N., Charrier, K., Sedger, L., Willis, C.R., et al. (2000). Reversible defects in natural killer and memory CD8 T cell lineages in interleukin 15-deficient mice. J. Exp. Med. *191*, 771–780.

Khan, T.N., Mooster, J.L., Kilgore, A.M., Osborn, J.F., and Nolz, J.C. (2016). Local antigen in nonlymphoid tissue promotes resident memory CD8+ T cell formation during viral infection. J. Exp. Med. *213*, 951–966.

Kimura, K., Kimura, D., Matsushima, Y., Miyakoda, M., Honma, K., Yuda, M., and Yui, K. (2013). CD8+ T cells specific for a malaria cytoplasmic antigen form clusters around infected hepatocytes and are protective at the liver stage of infection. Infect. Immun. *81*, 3825–3834.

Klonowski, K.D., Williams, K.J., Marzo, A.L., Blair, D.A., Lingenheld, E.G., and Lefrançois, L. (2004). Dynamics of blood-borne CD8 memory T cell migration in vivo. Immunity *20*, 551–562.

Krieg, A.M. (2006). Therapeutic potential of Toll-like receptor 9 activation. Nat. Rev. Drug Discov. *5*, 471–484.

Lau, L.S., Fernandez-Ruiz, D., Mollard, V., Sturm, A., Neller, M.A., Cozijnsen, A., Gregory, J.L., Davey, G.M., Jones, C.M., Lin, Y.H., et al. (2014). CD8+ T cells from a novel T cell receptor transgenic mouse induce liver-stage immunity that can be boosted by blood-stage infection in rodent malaria. PLoS Pathog. *10*, e1004135.

Lee, W.Y., and Kubes, P. (2008). Leukocyte adhesion in the liver: distinct adhesion paradigm from other organs. J. Hepatol. *48*, 504–512.

Liehl, P., Zuzarte-Luís, V., Chan, J., Zillinger, T., Baptista, F., Carapau, D., Konert, M., Hanson, K.K., Carret, C., Lassnig, C., et al. (2014). Host-cell sensors for Plasmodium activate innate immunity against liver-stage infection. Nat. Med. *20*, 47–53.

Mackay, L.K., Stock, A.T., Ma, J.Z., Jones, C.M., Kent, S.J., Mueller, S.N., Heath, W.R., Carbone, F.R., and Gebhardt, T. (2012). Long-lived epithelial immunity by tissue-resident memory T (TRM) cells in the absence of persisting local antigen presentation. Proc. Natl. Acad. Sci. USA *109*, 7037–7042.

Mackay, L.K., Rahimpour, A., Ma, J.Z., Collins, N., Stock, A.T., Hafon, M.L., Vega-Ramos, J., Lauzurica, P., Mueller, S.N., Stefanovic, T., et al. (2013). The developmental pathway for CD103(+)CD8+ tissue-resident memory T cells of skin. Nat. Immunol. *14*, 1294–1301.

Mackay, L.K., Braun, A., Macleod, B.L., Collins, N., Tebartz, C., Bedoui, S., Carbone, F.R., and Gebhardt, T. (2015). Cutting edge: CD69 interference with sphingosine-1-phosphate receptor function regulates peripheral T cell retention. J. Immunol. *194*, 2059–2063.

Masopust, D., Choo, D., Vezys, V., Wherry, E.J., Duraiswamy, J., Akondy, R., Wang, J., Casey, K.A., Barber, D.L., Kawamura, K.S., et al. (2010). Dynamic T cell migration program provides resident memory within intestinal epithelium. J. Exp. Med. *207*, 553–564.

Matsuda, J.L., Naidenko, O.V., Gapin, L., Nakayama, T., Taniguchi, M., Wang, C.R., Koezuka, Y., and Kronenberg, M. (2000). Tracking the response of natural killer T cells to a glycolipid antigen using CD1d tetramers. J. Exp. Med. *192*, 741–754.

McNamara, H.A., Cai, Y., Wagle, M.V., Sontani, Y., Roots, C.M., Miosge, L.A., O'Connor, J.H., Sutton, H.J., Ganusov, V.V., Heath, W.R., et al. (2017). Up-regulation of LFA-1 allows liver-resident memory T cells to patrol and remain in the hepatic sinusoids. Sci. Immunol. *2*, eaaj1996.

Miller, J.L., Sack, B.K., Baldwin, M., Vaughan, A.M., and Kappe, S.H. (2014). Interferon-mediated innate immune responses against malaria parasite liver stages. Cell Rep. *7*, 436–447.

Mueller, S.N., Heath, W., McLain, J.D., Carbone, F.R., and Jones, C.M. (2002). Characterization of two TCR transgenic mouse lines specific for herpes simplex virus. Immunol. Cell Biol. *80*, 156–163.

Murray, H.W., Luster, A.D., Zheng, H., and Ma, X. (2016). Gamma Interferon-Regulated Chemokines in Leishmania donovani Infection in the Liver. Infect. Immun. *85*, e00824-16.

Muschaweckh, A., Buchholz, V.R., Fellenzer, A., Hessel, C., König, P.A., Tao, S., Tao, R., Heikenwälder, M., Busch, D.H., Korn, T., et al. (2016). Antigen-dependent competition shapes the local repertoire of tissue-resident memory CD8+ T cells. J. Exp. Med. *213*, 3075–3086.

Muzumdar, M.D., Tasic, B., Miyamichi, K., Li, L., and Luo, L. (2007). A global double-fluorescent Cre reporter mouse. Genesis *45*, 593–605.

Nakanishi, Y., Lu, B., Gerard, C., and Iwasaki, A. (2009). CD8(+) T lymphocyte mobilization to virus-infected tissue requires CD4(+) T-cell help. Nature *462*, 510–513.

Pasparakis, M., Alexopoulou, L., Episkopou, V., and Kollias, G. (1996). Immune and inflammatory responses in TNF alpha-deficient mice: a critical requirement for TNF alpha in the formation of primary B cell follicles, follicular dendritic cell networks and germinal centers, and in the maturation of the humoral immune response. J. Exp. Med. *184*, 1397–1411.

Pircher, H., Bürki, K., Lang, R., Hengartner, H., and Zinkernagel, R.M. (1989). Tolerance induction in double specific T-cell receptor transgenic mice varies with antigen. Nature *342*, 559–561.

Ramakrishnan, C., Delves, M.J., Lal, K., Blagborough, A.M., Butcher, G., Baker, K.W., and Sinden, R.E. (2013). Laboratory maintenance of rodent malaria parasites. Methods Mol. Biol. *923*, 51–72.

Sacher, T., Knolle, P., Nichterlein, T., Arnold, B., Hämmerling, G.J., and Limmer, A. (2002). CpG-ODN-induced inflammation is sufficient to cause T-cell-mediated autoaggression against hepatocytes. Eur. J. Immunol. *32*, 3628–3637.

Samulowitz, U., Weber, M., Weeratna, R., Uhlmann, E., Noll, B., Krieg, A.M., and Vollmer, J. (2010). A novel class of immune-stimulatory CpG oligodeoxynucleotides unifies high potency in type I interferon induction with preferred structural properties. Oligonucleotides *20*, 93–101.

Schenkel, J.M., and Masopust, D. (2014). Tissue-resident memory T cells. Immunity *41*, 886–897.

Schenkel, J.M., Fraser, K.A., and Masopust, D. (2014). Cutting edge: resident memory CD8 T cells occupy frontline niches in secondary lymphoid organs. J. Immunol. *192*, 2961–2964.

Schenkel, J.M., Fraser, K.A., Casey, K.A., Beura, L.K., Pauken, K.E., Vezys, V., and Masopust, D. (2016). IL-15-Independent Maintenance of Tissue-Resident and Boosted Effector Memory CD8 T Cells. J. Immunol. *196*, 3920–3926.

Steinert, E.M., Schenkel, J.M., Fraser, K.A., Beura, L.K., Manlove, L.S., Igyártó, B.Z., Southern, P.J., and Masopust, D. (2015). Quantifying Memory CD8 T Cells Reveals Regionalization of Immunosurveillance. Cell *161*, 737–749.

Tohyama, M., Sayama, K., Komatsuzawa, H., Hanakawa, Y., Shirakata, Y., Dai, X., Yang, L., Tokumaru, S., Nagai, H., Hirakawa, S., et al. (2007). CXCL16 is a novel mediator of the innate immunity of epidermal keratinocytes. Int. Immunol. *19*, 1095–1102.

Tse, S.W., Radtke, A.J., Espinosa, D.A., Cockburn, I.A., and Zavala, F. (2014). The chemokine receptor CXCR6 is required for the maintenance of liver memory $CD8^+$ T cells specific for infectious pathogens. J. Infect. Dis. *210*, 1508–1516.

Wakim, L.M., Woodward-Davis, A., and Bevan, M.J. (2010). Memory T cells persisting within the brain after local infection show functional adaptations to their tissue of residence. Proc. Natl. Acad. Sci. USA *107*, 17872–17879.

Wakim, L.M., Woodward-Davis, A., Liu, R., Hu, Y., Villadangos, J., Smyth, G., and Bevan, M.J. (2012). The molecular signature of tissue resident memory CD8 T cells isolated from the brain. J. Immunol. *189*, 3462–3471.

Wuttge, D.M., Zhou, X., Sheikine, Y., Wågsäter, D., Stemme, V., Hedin, U., Stemme, S., Hansson, G.K., and Sirsjö, A. (2004). CXCL16/SR-PSOX is an interferon-gamma-regulated chemokine and scavenger receptor expressed in atherosclerotic lesions. Arterioscler. Thromb. Vasc. Biol. *24*, 750–755.

STAR★METHODS

KEY RESOURCES TABLE

REAGENT or RESOURCE	SOURCE	IDENTIFIER
Antibodies		
Rat monoclonal anti-CD8α (clone 53-6.7)	Biolegend	Cat#100748, RRID: AB_2562100
Rat monoclonal anti-CD8α (clone 53-6.7)	BD	Cat# 553035, RRID: AB_398527
Rat monoclonal anti-CD44 (clone IM7)	Biolegend	Cat# 103026, RRID: AB_493713
Rat monoclonal anti-CD62L (clone MEL-14)	Biolegend	Cat# 104432, RRID: AB_2285839
Armenian Hamster monoclonal anti-CD69 (clone H1.2F3)	eBioscience	Cat# 15-0691-82, RRID: AB_468772
Rat monoclonal anti-Vα8.3 (clone B21.14)	BD	Cat# 553377, RRID: AB_394821
Rat monoclonal anti-Vα2 (clone B20.1)	BD	Cat# 560624, RRID: AB_1727584
Parasite Strains		
Plasmodium berghei	The Malaria Research and Reference Reagent Resource Center; BEI resources	MRA-871
Plasmodium berghei ANKA-OVA	Kimura et al., 2013	N/A
Peptides and Recombinant Proteins		
SIINFEKL, SSIEFARL, KAVYNATC peptides	Auspep	N/A
Recombinant human IL-2	Peprotech	Cat# 200-02
Recombinant mouse IL-15	*In vitro* Technologies	Cat# 447-ML
Experimental Models: Mouse lines		
C57BL/6	Animal Resources Centre	Stock # 000664
OT-I	Hogquist et al., 1994	N/A
gBT-I	Mueller et al., 2002	N/A
PbT-I	Lau et al., 2014	N/A
P14	Pircher et al., 1989	N/A
Ly5.1/IL-15$^{-/-}$	Kennedy et al., 2000	N/A
Experimental models: Organisms/Strains		
Anopheles stephensi	The Malaria Research and Reference Reagent Resource Center; BEI resources	Strain: STE2/MRA-128
Recombinant DNA		
CpG 2006-21798	Geneworks	Fernandez-Ruiz et al., 2016
CpG 2006-21798	Integrated DNA Technologies	Fernandez-Ruiz et al., 2016
Software and Algorithms		
Imaris v9.1	Bitplane	http://www.bitplane.com/
Prism v7	GraphPad	https://www.graphpad.com/scientific-software/prism/
FlowJo v9.9	Tree Star	https://www.flowjo.com/
Diva	BD Bioscience	N/A

CONTACT FOR REAGENT AND RESOURCE SHARING

Further information and requests for resources and reagents should be directed to and will be fulfilled by the Lead Contact, William Heath (wrheath@unimelb.edu.au).

EXPERIMENTAL MODEL AND SUBJECT DETAILS

Mice

C57BL/6 (B6), gBT-I (Mueller et al., 2002), OT-I (Hogquist et al., 1994), PbT-I (Lau et al., 2014), P14 (Pircher et al., 1989), TdTomato (Muzumdar et al., 2007), IFNαR2−/− (Fenner et al., 2006), TNF$^{-/-}$ (Pasparakis et al., 1996), Sting$^{-/-}$ (Jin et al., 2011), IFN-γ$^{-/-}$ (Dalton et al., 1993), Ly5.1/IL-15$^{-/-}$ (Kennedy et al., 2000) and Stat6$^{-/-}$ (Kaplan et al., 1996) mice were bred and maintained at the Department of Microbiology and Immunology, The University of Melbourne. Des-TCR and Des-RAG (Hua et al., 1986) mice were bred and maintained at the Centenary Institute. All mice used were 6-12 weeks of age and littermates of the same sex were randomly assigned to experimental groups. Animals used for the generation of the sporozoites were 4-5 week old male Swiss Webster mice purchased from the Monash Animal Services (Melbourne, Victoria, Australia) and housed at 22° to 25°C on a 12 hr light/dark cycle at the School of Biosciences, The University of Melbourne, Australia.

Ethics statement

All animal experiments were in accordance with the Prevention of Cruelty to Animals Act 1986, the Prevention of Cruelty to Animals Regulations 2008 and the National Health and Medical Research Council (2013) Australian code for the care and use of animals for scientific purposes. The protocols were approved by the Melbourne Health Research Animal Ethics Committee, University of Melbourne (ethics protocols IDs: 1513505, 1513470) and by the Royal Prince Alfred Hospital Sydney local health district Animal Ethics Committee (ethics protocol ID: 2014/001).

Plasmodium Infection

Anopheles stephensi mosquitoes (STE2, MRA-128, from BEI Resources) were reared in an Australian Biosecurity (Department of Agriculture and Water Resources) approved insectary (Benedict, 1997). The conditions were maintained at 27°C and 75%–80% humidity with a 12 h light and dark photo-period in filtered drinking water (Frantelle beverages, Australia) and fed with Sera vipan baby fish food (Sera). The larvae were bred in plastic food trays (P.O.S.M Pty Ltd, Australia) containing 300 larvae, each with regular water changes every 3 days. Upon ecloding, the adult mosquitoes were transferred to aluminum cages (BioQuip Products, Inc. St.Rancho Dominguez, CA, USA) and kept in a secure incubator (Conviron), in the insectary at the same temperature and humidity and maintained on 10% sucrose.

P. berghei ANKA wild-type Cl15cy1 (BEI Resources, NIAID, NIH: MRA-871, contributed by Chris J. Janse and Andrew P. Waters) and PbA expressing OVA under the HSP70 promoter were used (Kimura et al., 2013). Infections of naive Swiss mice were carried out by i.p inoculation of PbA infected RBCs obtained from a donor mouse between the first and fourth passages from a cryopreserved stock. Parasitemia was monitored by Giemsa smear and exflagellation quantified 3 days post infection. 1 μL of tail prick blood was mixed with 100 μL of exflagellation media (RPMI [Invitrogen] supplemented with 10%v/v fetal bovine serum, pH 8.4), incubated for 15 min at 20°C, and exflagellation events per 1x10^4 red blood cells were counted. *A. stephensi* mosquitoes were allowed to feed on anaesthetised mice once the exflagellation rate was assessed between 12-15 exflagellation events per 1x10^4 red blood cells. 22 days after biting, salivary glands were dissected and checked for the presence of sporozoites.

Sporozoites were dissected from mosquito salivary glands (Ramakrishnan et al., 2013), resuspended in cold PBS, and either left untreated for challenge experiments or irradiated with 20,000 rads using a gamma 60Co source. For challenge experiments, 200 freshly dissected PbA sporozoites were injected i.v. as indicated. Mice were assessed for parasitemia at day 6, 7, 8, 10 and 12 using flow cytometry. Briefly, a drop of blood was collected from the mice and stained with Hoechst 33258 dye (ThermoFisher, Scoresby, Victoria, Australia) for 1 hr at 37°C. Samples were analyzed on a LSR Fortessa (BD Biosciences, San Diego, USA) using a violet laser (405 nm) to excite the dye. After gating on RBCs the percentage of Hoechst positive cells were measured. Values were compared to uninfected controls and typically values of > 0.1% were considered positive for parasites. Mice positive for parasites on two consecutive days were euthanized. Mice were considered sterilely protected if they remained parasitemia-negative on day 12 after challenge.

METHODS DETAILS

Vaccination

For vaccinations with radiation attenuated sporozoites (RAS), B6 mice were injected i.v. with 50,000 RAS. Vaccination using infection and treatment was achieved by infecting mice intravenously with 10^6 PbA infected RBC (iRBC). After infection, mice were injected intraperitoneally with 0.8 mg chloroquine daily from day 4 to day 8, followed by 600 mg/L chloroquine in drinking water on day 9 and day 10.

Naive OT-I, gBT-I and PbT-I CD8$^+$ T cells were isolated by negative selection from the lymph nodes and/or spleen as previously described (Fernandez-Ruiz et al., 2016). Briefly, tissues were disrupted by passing through 70 μm cell strainers and red cells lysed. Single cell suspensions were labeled with a cocktail of rat monoclonal antibodies specific for CD4, MHC Class II, macrophages and neutrophils prior to incubating with BioMag goat anti-rat IgG beads (QIAGEN, Chadstone, VIC, Australia) and separating using a magnet. Enriched naive CD8$^+$ T cells were counted and their purity analyzed by staining with anti-CD8 and anti-Vα TCR antibodies. Cell counts were adjusted to 2.5x10^5/mL in PBS and mice were injected with 200 μL i.v.. For HSV studies, mice were infected by

skin scarification with 10^6 PFU HSV-1 following the transfer of 10^6 gBT-I cells as described (Gebhardt et al., 2009). Naive OT-I cells were primed in B6 mice by i.v injection of 5 nmol of CpG 2006-21798 (Krieg, 2006; Fernandez-Ruiz et al., 2016) and 2 μg of anti-Clec9A antibody genetically fused to ovalbumin (Caminschi et al., 2008).

In vitro T cell activation and transfer

OT-I (Ly5.1 or uGFP) cells were activated *in vitro* for 4-5 days using naive B6 splenocytes coated with 0.5 μg/mL of SIINFEKL peptide (Auspep, Tullamarine, VIC, Australia) in complete media (RPMI containing 10% FCS, 2 mM L-glutamine, 5 mM HEPES and 50 μM 2-mercaptoethanol (Sigma Aldrich, Castle Hill, NSW, Australia)). OT-I cells were activated in the presence or absence of 5 μg LPS (Sigma), 10 U/mL of recombinant human IL-2 (Peprotech, Mt Waverly, VIC, Australia) or 50 ng/mL rmIL-15 (*In Vitro* Technologies, Noble Park, VIC, Australia). gBT-I (Ly5.1 or uGFP) cells and P14.Thy1.1 cells were activated *in vitro* for 4-5 days in complete media using naive B6 splenocytes coated with 0.1 μg/mL of SSIEFARL peptide or KAVYNATC peptide, respectively. Cells were activated in the presence of 6 μg of LPS (Sigma), with 12.5 U/mL of rhIL-2 added at day 3 and day 4. Prior to transfer the cells were washed extensively with PBS to remove any excess LPS, counted and their purity analyzed by staining with antibodies against CD8 and the relevant Vα TCR. Activated cells were adjusted to the required concentration and injected in a volume of 200 μL of PBS via the tail vein. In experiments where cells were transferred in the presence of adjuvants, the cells were mixed with 50 μg of poly I:C or 75.3 μg of CpG 1668 (CpG B) or CpG 2006-21798 (CpG B-P) (Geneworks, Thebarton, SA, Australia) (Fernandez-Ruiz et al., 2016) per mouse.

Lymphocyte isolation from organs

Tissues were harvested from mice at different time points after immunization. For spleen cell preparations, the organ was passed through 70 μm mesh and red blood cells were lysed. Liver cell suspensions were passed through 70 μm mesh and resuspended in 35% isotonic Percoll (Sigma). Cells were then centrifuged at 500 g for 20 min at room temperature (RT), the pellet harvested and then red cells lysed before further analysis.

Flow cytometry

Cells were labeled with monoclonal antibodies specific for CD8α (53-6.7), Vα2 (B20.1), Vα8.3 (B21.14), Vβ5.1/5.2 (MR9-4), Vβ8.1/8.2 (MR5-2), Vβ10 (B21.5) from BD, KLRG1 (2F1), CD44 (IM7), CD62L (MEL-14), CD45.1 (A20), CD45.2 (104), NK1.1 (PK136) from Biolegend (Australian Biosearch, Karrinyup, WA. Australia), CD69 (H1.2F3) and CD101 (Moushi101) from eBioscience (Jomar Life Research, Scoresby, VIC, Australia) and Des-TCR (Desiré clonotypic antibody, purified and conjugated with biotin in house at the Centenary Institute). The cells were stained at 4°C for 20 min, washed, and analyzed without fixation. Intracellular staining for PLZF (9E12) was performed after surface staining with a CD1d α-GalCer tetramer (Hammond et al., 2001; Matsuda et al., 2000) using the Transcription factor fixation/permeabilization buffer kit according to the manufacturer's instructions (Biolegend). Dead cells were excluded by propidium iodide staining or far red live/dead fixable dye (ThermoFisher). Single-color positive control samples were used to adjust compensation and cells were analyzed by flow cytometry on a LSR Fortessa (BD Biosciences), using Flowjo software (Tree Star Inc.).

Intravital 2 photon microscopy

Mice were anaesthetized with isoflurane (Cenvet; 2.5% for induction, 1.5% for maintenance, vaporized in an 80:20 mixture of oxygen and air) using a Tech 3 vaporizer (Surgivet) and the abdomen shaved. The liver was surgically exposed as previously described (Fernandez-Ruiz et al., 2016). Briefly, a circular incision was made in the skin 5-7 mm below the diaphragm. The lateral peritoneal vessel was embolized by clamping for 4 min using 2 forceps, held approximately 5 mm apart. An incision was then made across the embolized blood vessel, through the peritoneal membrane to expose the caudal lobe of the liver. Mice were then positioned in a custom-made imaging stage and the region around the exposed liver covered in PBS-moistened gauze to prevent dehydration. The liver was then attached to a glass coverslip using drops of super glue placed at the periphery of the exposed tissue.

Images were acquired with an upright LSM710 NLO multiphoton microscope (Carl Zeiss Microimaging) or FVMPE-RS multiphoton microscope (Olympus) enclosed in a custom-built environmental chamber (Precision Plastics) that was maintained at 35°C with heated air. Images were acquired with a 20X/1.0 NA water immersion objective. Fluorescence excitation was provided by a Chameleon Vision II Ti:Sapphire laser (Coherent), with dispersion correction on the LSM710. EGFP and TdTomato were excited at 890 nm. For image acquisition on the FVMPE-RS microscope, fluorescence excitation was provided by a Mai Tai (690-1040 nm) laser or an Insight laser (690-1300nm) (Spectra Physics). EGFP was excited at 910 nm using the MaiTai laser and TdTomato was excited at 1125 nm using the Insight laser. For four-dimensional datasets, three-dimensional stacks were captured every 30 s. Raw imaging data were processed with Imaris 9.1 (Bitplane). Cell migration was analyzed through automatic cell tracking aided by manual corrections. Data were used to plot graphs in Prism 7 (GraphPad software). For the generation of movies, image sequences exported from Imaris were composed in Adobe After Effects.

QUANTIFICATION AND STATISTICAL ANALYSIS

Statistical analysis

Figures were generated using GraphPad Prism 7. Data are shown as mean values ± SEM or mean ± SD as indicated in the figure legends. Data was log transformed, assessed for normality then either Student's t tests, Mann-Whitney rank sum U test, one way ANOVA or Kruskal Wallis test was performed depending on whether the data was normally distributed. Dunn's multiple comparison post-test was used to compare data not normally distributed while Tukey's multiple comparison test was used to compare normally distributed data. The statistical tests performed on the data are indicated in the figure legends and results, along with sample size indicating the number of animals used. P values < 0.05 (*), < 0.01 (**) or 0.001 (***) were considered statistically significant.